Published in final edited form as:
Clin Cancer Res. 2009 December 15; 15(24): 7529–7537. doi:10.1158/1078-0432.CCR-09-0336.

RNA Interference Screen Identifies VEGFR1 as Potentially Synthetic Lethal to Aberrant Wnt/β-catenin Activation in Colon Cancer

Snehal Naik, **Robin S. Dothager**, **Jayne Marasa**, **Cory L. Lewis**, and **David Piwnica-Worms**[1]
Molecular Imaging Center, Mallinckrodt Institute of Radiology, and Department of Developmental Biology, Washington University School of Medicine, St. Louis, MO 63110

Abstract

Purpose: The Wnt/β-catenin (β-cat) signaling cascade is a key regulator of development, and dysregulation of Wnt/β-cat contributes to selected cancers, such as colorectal, breast and hepatocellular carcinoma, through abnormal activation of Wnt target genes. To identify novel modulators of the Wnt/β-cat pathway which may emerge as therapeutic targets, we performed an unbiased high-throughput RNA interference screen.

Experimental Design: A synthetic oligonucleotide siRNA library targeting 691 known and predicted human kinases was screened in Wnt3a-stimulated human cells in a live cell luciferase assay for modulation of Wnt/β-cat-dependent transcription. Follow-up studies of a selected high-confidence "hit" were conducted.

Results: A robust quartile-based statistical analysis and secondary screen yielded several kinases worthy of further investigation, including Cdc2L1, Lmtk3, Pank2, ErbB3, and of note, vascular endothelial growth factor receptor-1 (VEGFR1/Flt1), a receptor tyrosine kinase with putative weak kinase activity conventionally believed to be a negative regulator of angiogenesis. A series of loss-of-function, genetic null, and VEGFR tyrosine kinase inhibitor assays further revealed that VEGFR1 is a positive regulator of Wnt signaling that functions in a glycogen synthase kinase-3β (GSK3β)-independent manner as a potential synthetic lethal target in Wnt/β-cat-addicted colon carcinoma cells.

Conclusion: This unanticipated non-endothelial link between VEGFR1 tyrosine kinase activity and Wnt/β-cat signaling may refine our understanding of aberrant Wnt signaling in colon carcinoma and points to new combinatorial therapeutics targeted to the tumor cell compartment, rather than angiogenesis, in the context of colon cancer.

Keywords

siRNA; high throughput screen; synthetic lethality; phosphorylation; bioluminescence; colon cancer

Introduction

The Wnt signal transduction cascade relays pro-growth signals through β-cat, a key transcriptional co-activator, whose cellular levels are tightly-regulated. In non-active states, serine/threonine phosphorylation of β-cat by GSK3β, the component kinase of the adenomatous polyposis coli (APC)-mediated destruction complex, results in β-cat

1Correspondence should be addressed to D.P-W. at: piwnica-wormsd@mir.wustl.edu. Mailing address: Mallinckrodt Institute of Radiology, Washington University School of Medicine, 510 S. Kingshighway Blvd., Box 8225, St. Louis, MO 63110 Phone: (314) 362-9359, Fax: (314) 362-0152.

polyubiquitination mediated by the E3-ligase, β-TrCP, and consequent proteasomal degradation. In the presence of activating Wnt ligands, the destruction complex is inhibited and an active β-cat population accumulates in the cytoplasm and translocates into the nucleus, where it forms a transactivator complex with lymphoid enhancing factor (LEF) or T-cell factor (TCF), resulting in the transcription of over 50 target genes (1,2). Aberrant activation of the Wnt pathway, resulting in ligand-independent signaling and constitutively high levels of Wnt target gene expression is common in colon cancers (1,2). Although such Wnt/β-cat activation contributes to certain forms of cancer, it may also create therapeutically exploitable vulnerabilities within the context of synthetic lethality (3,4). Two genes are classically synthetic lethal if cells with a mutation in either one of the genes are viable, but simultaneous mutation of both genes causes death or impairs cellular fitness (5,6). The idea can be extended to common mechanisms of cancer transformation, such as gain-of-function oncogenes exemplified by aberrant Wnt/β-cat activation. In this regard, inhibition or mutation of a second gene may be lethal or anti-proliferative only in the context of specific oncogenic up-regulation (3). Thus, it may be possible to use the contextual difference of aberrant Wnt/β-cat activation to find selective targets for therapeutic intervention. Kinases, an important family of functional regulators, have emerged as therapeutically-alluring targets since single kinase inhibition can often eliminate an entire stimulatory or inhibitory arm of a signal transduction cascade. We have generated a screening strategy that combines the study of Wnt pathway activation with loss of individual kinases to uncover candidate kinase modulators that may emerge as therapeutic targets in the context of Wnt-addicted colon cancer.

Materials and Methods

Cell lines and reagents

pCMV-FLuc has been previously described (7). *pTOPFLASH* and *pcDNA3.1* were purchased from Upstate Products and Invitrogen Corporation, respectively. STF293 reporter cells were kindly provided by Dr. Jeremy Nathans (Johns Hopkins University School of Medicine) and cultured in STF293 medium. HEK293, HEK293T and HeLa cells (ATCC) were cultured in DMEM supplemented with 10% heat-inactivated fetal bovine serum (ΔFBS) and 1% glutamine. SW480 and KM12L4a colon carcinoma cells (kindly provided by Dr. Loren Michel, Washington University School of Medicine) were cultured in DMEM supplemented with 10% FBS and 1% glutamine. L cells and L Wnt-3a cells were purchased from ATCC and conditioned medium collected as per the ATCC protocol. A HEK293 cell line stably expressing FLuc (293Luc) was established by transfecting 293 cells with *pCMV-FLuc* using FuGENE 6 transfection reagent (Roche) for 48 hours followed by selection of single colonies after continuous exposure to G418 (0.4 mg/mL). SB216763 (Sigma-Aldrich) and VEGFR-TK inhibitors II and III (EMD Biosciences) were reconstituted in DMSO. Plasmids expressing shRNA sequences were provided by the Genome Sequencing Center, Washington University School of Medicine. Each sequence was provided in a *pLKO.1* expression vector.

High-throughput screening

siRNA screening was performed in black, clear-bottomed, 96-well culture plates (Corning 3904) using a Beckman-Coulter Core robotics system, including an FX liquid handler, controlled by the Sagian graphical method development tool (SAMI scheduling software). STF293 cells (10,000/well) in STF293 medium (DME/F12 supplemented with 10% ΔFBS and 1% glutamine) at 100 μl/well were seeded one day before transfection. Plates were maintained in an environmentally controlled Cytomat incubator until needed for operations, thereby optimizing health and uniform treatment of all plates.Forward transfection was performed with a 96 multichannel head on the FX liquid handler, adding 0.2 μl/well of media-complexed Dharmafect1 reagent (Dharmacon Research Inc.) to the aliquotted siRNA library (Kinase siRNA set v2; Qiagen Inc.) in a 96-well reaction plate. Experimental siRNA oligos were

arrayed in columns 2-11 of each plate and individual controls comprising mock-transfected wells, a non-targeting siCONTROL sequence (siC, Dharmacon Research Inc.), as well as a Firefly luciferase-targeting siRNA sequence (Dharmacon Research Inc.) were placed manually in columns 1 and 12. After incubation of siRNA-Dharmafect1 complexes for 20 min at RT, 100 μl of the complexed siRNA was added to each well of a plate with cells (x 3 plates) using the FX liquid handler, yielding a final concentration of ~25 nM siRNA/well. Plates were maintained in the Cytomat for 24 hrs, after which each plate was aspirated using the Bio-Tek EL405 Select plate washer. 200 μl/well Wnt3a-conditioned media containing 150 μg/mL D-luciferin (D-Luc) (Biosynth) was added using the FX liquid handler and cells were incubated for 10 mins. Luminescent signal was measured in ultrasensitive detection mode on an EnVision plate reader (PerkinElmer) 10 mins, 6 hrs, 12 hrs and 18 hrs post Wnt3a addition. Cell viability was then determined with resazurin dye (Sigma R7017) (final conc., 44 μM)) after a 90 min incubation at 37°C as monitored on a FLUOstar OPTIMA fluorescence reader (BMG Labtech; excitation, 544 nm, emission, 590 nm).

Secondary shRNA screen

STF293 cells in DME/F12 media supplemented with 10% ΔFBS and 1% glutamine were plated in 24 or 96 well plates one day before transfection such that cells would be ~70% confluent on the day of transfection. In quadruplicate, cells were transfected with 800 ng (for 24 well plate) or 300 ng (for 96 well plate) of shRNA expression vector. Four individual shRNA sequences (except three for Pank2) that targeted non-overlapping segments of the coding region of each original high stringency “hit” gene were used. Also included were a non-targeting scrambled sequence (negative control) and a sequence targeting Firefly luciferase (positive control). Plasmids were transfected using Lipofectamine 2000 at a 2.5:1 ratio (volume of reagent to micrograms of DNA) in 100 μL (for 24 well plates) or 50 μL (for 96 well plates) of serum-free DME/F12 media. Transfection reagent was added to serum-free media and incubated for 5 min followed by addition of DNA. After incubation for 20 min, transfection mixture was added drop-wise to wells of assay plates. Cells were incubated in transfection mixture for 4 hrs and then media was replaced with fresh DME/F12 media containing serum. After transfection, cells were incubated for 24 hrs followed by doubling the volume in each well by addition of Wnt3a-conditioned media that contained 150 μg/mL of D-Luciferin. Cells were incubated for another 24 hrs and then imaged on a bioluminescence imaging system (IVIS 100, Caliper; filter, open; f-stop, 1; exposure, 5 min; binning, 8). After bioluminescence imaging, an MTS cell viability assay was performed (CellTiter 96 AQueous One Solution Cell Proliferation Assay, Promega) by measuring formation of the formazan product (absorbance at 490 nm, 1 hr, 37°C) using a FluoStar Optima plate reader for 24 well plates or an EL 311 plate reader (BioTek) for 96 well plates.

RT^2 Profiler PCR Wnt Array

Embryonic stem (ES) cells from wild-type R1 or *VEGFR1/Flt1*$^{(-/-)}$ mice were provided by Dr. Guo-Hua Fong (University of Connecticut Health Center) and Dr. Kyunghee Choi (Washington University School of Medicine) and maintained at the Murine Embryonic Stem Cell Core at Washington University. Cells were cultured in DMEM containing fetal calf serum, L-glutamine, non-essential amino acids, HEPES, leukemia inhibitory factor and 2-mercaptoethanol, and plated on gelatinized 10-cm tissue culture dishes to eliminate MEFs before experimental assays. Following incubation of ES cells in the presence or absence of rWnt3a, RNA was obtained using the RNeasy RNA extraction kit (Qiagen), including the optional DNase digestion protocol. RT-PCR array profiling was performed using the pathway-specific RT^2 Profiler PCR Array system (Superarray) as per the manufacturer's instruction, in an ABI 7300 real-time PCR system (Applied Biosystems). Data analysis using the ΔC_t method was performed as per a data analysis template available online.[1] Briefly, ΔC_tvalues were calculated by subtracting average cycle threshold (C_t) values for housekeeping genes (GAPDH,

β-actin and Hprt1) from C_t values for T (Brachyury). Fold-differences were calculated as $2^{-\Delta C}$t (rWnt3a treated) / $2^{-\Delta C}$t (untreated) for both wild type and *VEGFR1*$^{(-/-)}$ ES cells.

Semi-quantitative RT-PCR

siRNA transfections were performed as above and allowed to proceed for 48 hrs. RNA was extracted using a RNeasy RNA extraction kit (Qiagen). One-step RT-PCR was performed according to the manufacturer's protocol using an Access RT-PCR System (Promega Corporation) on a Gene Amp® 2700 PCR system (Applied Biosystems). Primer sequences were as follows: VEGFR1 extracellular domain, forward primer TGGGACAGTAGAAAGGGCTT, reverse primer GGTCCACTCCTTACACGACAA; GAPDH, forward primer GTGAAGGTCGGAGTCAACGG, reverse primer TGATGACAAGCTTCCCGTTCTC. Amplified products were subjected to agarose gel electrophoresis and visualized as a 384 bp product for VEGFR1 and a 200 bp product for GAPDH using a ChemiImager® (Alpha Innotech Corp.).

In cellulo transfection assays

In STF293 cells, follow-up siRNA validation studies were performed using a forward transfection protocol with Dharmafect1 reagent (Dharmacon Research Inc.) at a final concentration of 50 nM siRNA (ON-TARGET PLUS SMARTPool, L-003136-00; Dharmacon Research Inc.), and 20 nM siRNA (individual duplexes; Dharmacon Research Inc.). In other experiments, colon carcinoma cells were transfected with *pTOPFLASH* using Lipofectamine 2000 (Invitrogen) as per the manufacturer's instructions. Bioluminescence was captured using an IVIS 100 or IVIS 50 imaging system and LivingImage (Caliper Lifesciences) and Igor (Wavemetrics) software. Acquisition parameters were as follows: no filter; exposure time, 1-2 min; binning, 8; f-stop, 1; FOV, 12 cm (IVIS 50) or 10 cm (IVIS 100).

MTS assays

1000 cells/ well of STF293, HeLa, KM12l4a and SW480 cells were plated in appropriate media in clear 96-well plates. Numerous wells containing medium only were also plated as background controls. Each cell line was treated with increasing drug concentrations in triplicate, while STF293 cells were treated with Wnt3a together with increasing drug concentrations. Drug pre-treatment proceeded for 72 hrs, after which MTS reagent (Promega) was added, incubated 1-3 hrs depending on the cell line, and absorbance assayed at 490 nM in an EL 311 plate reader (Bio Tek Instruments). Background subtraction was performed from medium-only wells that had each been treated with the corresponding drug concentrations in duplicate, to calculate corrected absorbance. Data were then normalized as fold-drug untreated values for each cell type to facilitate plotting on the same graph.

Immunofluorescence and confocal microscopy

Cells were transfected (for siRNA assays) or treated (for Inh II assays) in 35 mm glass coverslip dishes (MatTek Cultureware) and treated with Wnt3a or control media for two hrs prior to fixation in 4% paraformaldehyde solution. Samples were then washed, treated with ice-cold methanol for 10 min at −20°C, washed and incubated with anti-β-cat antibody (BD Biosciences, 1:500 dilution) overnight at 4°C on a rocking platform. Following three washes, a 2-hr incubation in Alexa 488-conjugated secondary antibody (Invitrogen Corporation, 1:500 dilution) was performed at RT in the dark. Samples were incubated with 10 μg/mL of 4′,6-diamidino-2-phenylindole (DAPI) for 15 min in the dark and stored in PBS at 4°C protected from light. Images (10 μM slice thickness, 40X magnification) were acquired using an inverted Zeiss Axiovert 200 laser scanning confocal microscope coupled to a Zeiss LSM 5 PASCAL

[1]http://www.sabiosciences.com/pcrarraydataanalysis.php

fitted with excitation lasers at 488 nm (for β-cat) and 405 nm (for DAPI), and long pass emission filters 505 nm (for β-cat) and 420 nm (for DAPI).

Immunoprecipitation and Western blotting

Cells were transfected (for siRNA assays) or treated (for Inh II assays) in 10-cm tissue culture-treated dishes and harvested in IP buffer (50 mM HEPES, pH 7.5, 150 mM NaCl, 5% glycerol, 1% Triton X-100, 1 mM EDTA, 10 mM NaF and 30 mM glycerol phosphate) freshly combined with a 1:100 dilution of protease inhibitor cocktail (Sigma-Aldrich) and 200 μM final concentration of sodium orthovanadate. Protein amounts were quantified using a BCA assay (Pierce) according to manufacturer's protocol. 500 μg of protein from each sample was incubated for 1 hr with anti- β-cat antibody (BD Biosciences, 0.5 μg) on a rocking platform and then complexed with Protein A-agarose beads (Calbiochem) overnight at 4°C on a rotator. Samples were washed three times after centrifugation at 6000 rpm and boiled for 10 mins. before separation by SDS-PAGE. After transfer to a PVDF membrane, blocking was allowed to proceed for 2 hrs at RT, followed by incubation with anti-pTyr antibody (clone 4G10, Upstate Products; 1:1000 dilution) overnight at 4°C. Immune complexes were detected by horseradish-peroxidase-labeled secondary antibodies and enhanced chemiluminescence reagent (Amersham Biosciences). Exposure and densitometric analysis were performed using the IVIS imaging system and LivingImage (Caliper Lifesciences) and Igor (WaveMetrics) software. A similar SDS-Page and immunoblotting protocol was followed for detection of β-cat (1:200 dilution), VEGFR1 (1:200 dilution) and actin (1:1000 dilution) using antibodies from Santa Cruz, Chemicon Corporation and Sigma-Aldrich, respectively.

Statistical analysis and “hit” selection

In the primary siRNA screen, luminescence data acquired 18 hrs post Wnt3a treatment was normalized to cell viability data (expressed as value = x). Median (Q2), first (Q1) and third (Q3) quartile values were calculated for all normalized values and subjected to plate-by-plate analysis. To facilitate experiment-wide analysis, further normalization was performed with a control non-targeting siRNA placed on each individual assay plate. Q1, Q2 and Q3 values were calculated as above. Averages and SEM calculations were performed for triplicates of log[x/median] values. Upper and lower boundaries were calculated as $Q3 + 2c(Q3 - Q2)$ and $Q1 - 2c(Q2 - Q1)$, respectively, for $c = 1.7239$ corresponding to a high stringency targeted error rate ($\alpha = 0.0027$) and $c = 0.9826$ corresponding to a lower stringency targeted error rate ($\alpha = 0.046$) (8). High stringency “hits” were chosen as those targets that scored $\alpha \leq 0.0027$ in both a plate-by plate and an experiment-wide analysis. Selected targets clustered within the first two plates (numbers 1-150; red circles in Fig. 1) represented “hits” that scored as significant by high stringency criteria in an experiment-wide analysis only, but not by a plate-by-plate analysis (listed in Supplementary Table 3). This ensued from alphabetical clustering and non-random placement of siRNA sequences on the plates by the vendor, resulting in over-representation of “hits” in the first two plates, thereby infringing on the sparse-hit hypothesis which assumes that “hits” are randomly spaced throughout the dataset.

Experimental Statistical Analyses

Student's *t*-tests, two-way analysis of variance (ANOVA), curve-fitting, box plots and IC_{50} calculations were performed using Graph-pad software (Graphpad).

Results

Kinase-targeted high-throughput siRNA screen of Wnt/β-cat-dependent transcription

We used a synthetic oligonucleotide siRNA library targeting known and predicted human kinases in a high throughput screening format for systematic, yet unbiased target discovery in

contexts that were both physiologically relevant and therapeutically alluring (3,4). HEK293 cells stably expressing a luciferase transcriptional reporter of Wnt/β-cat target-gene activation (STF293 cells) (9) were transfected with 1382 siRNA duplexes targeting 691 distinct genes as a pool of two duplexes per target in a 96-well high throughput screen (Supplementary Fig. 1), and subsequently treated with Wnt3a-conditioned media (Wnt3a) (10) to emulate pathway activation. Human cells together with a functionally-targeted synthetic oligonucleotide library were used to maximize discovery of potential disease-relevant candidates, and minimize off-target effects such as those that can be observed in genome-wide screens conducted in model organisms (11,12). A highly stringent targeted error rate in a quartile-based analysis (8) (see Material and Methods) was employed to uncover candidates of statistical relevance (Fig. 1). Eleven kinases (Cdc2L1, Pank2, Lmtk3, Flt1, ErbB3, Fgr, Mapk10, Phkg1, Phkg2, Pbk, and Stk24), representing both serine/threonine and tyrosine kinases, were recovered as "hits", all of which were kinases not previously associated with the Wnt pathway (Supplementary Table 1). Importantly, analysis at lower stringency revealed additional kinases, several with known Wnt pathway regulatory functions (TGFβR, NLK, CK1/2, CDKN2a, AKT2/3, and GSK3α/β), which served to authenticate the screen (Supplementary Fig. 2; Supplementary Table 2). Also, a subset of kinases enriched in cell cycle regulators emerged from an experiment-wide analysis, including the noteworthy genes Cdk8 (13), ATM, and Plk3 (Supplementary Table 3). Loss of one subset of kinases (VEGFR1/Flt1, Pank2 and Lmtk3) resulted in reduced β-cat-dependent transcription (Fig. 1), representing potential targetable therapeutic genes.

Validation of hit genes using shRNA knock-down

To validate changes in Wnt/β-cat signaling that were observed in the primary screen, we re-screened in STF293 cells the eleven "hit" genes using four separate shRNA sequences corresponding to each gene of interest. Plasmids bearing shRNA were chosen for the secondary screen because of their potential for higher potency, fewer off-target effects, and stability. The shRNA sequences were selected for those that target non-overlapping segments of the coding regions of hit genes, and were assessed individually as opposed to being pooled, as was done in the primary siRNA screen. Genes were qualified as reproducible if, in at least two of three separate experiments, two or more shRNA sequences for a target gene increased or decreased luciferase signals above or below the median of a non-targeting negative control shRNA in concordance with the trend previously observed with siRNA (see Fig. 2, illustrating a representative experiment). Overall, shRNA against five of the original eleven hit genes showed the same effect on luciferase signal as was observed in the primary screen, and were deemed reproducible: Cdc2L1, Lmtk3, Pank2, ErbB3, and VEGFR1/Flt1. Only VEGFR1/Flt1 was concordant in all three independent experiments.

Characterization of VEGFR1/Flt1 as a "high confidence hit"

Direct therapeutic applications may be found for candidates whose loss-of-function by RNA interference results in attenuated Wnt/β-cat signaling, especially in the context of "oncogene-addicted" colon cancer cells where loss of aberrantly active Wnt/β-cat signaling results in decreased cell survival (14). In this regard, specific identification of VEGFR1/Flt1, but not VEGFR2/KDR or VEGFR3/Flt4, as a "reproducible hit" was striking. VEGFR1, a receptor tyrosine kinase (TK) with putative weak kinase activity, is thought conventionally to function as a negative regulator of angiogenesis (15,16), an endothelial cell process that is actively targeted in the treatment of colorectal cancers (17). To extend the cellular link between VEGFR1 function and Wnt/β-cat signal transduction, we further validated the effects of VEGFR1 knock-down on the β-cat-dependent transcription observed in the primary screen. Using STF293 cells, a pool of four independently-designed sequences against VEGFR1, as well as three of these four when tested as individual siRNA sequences, resulted in knock-down of VEGFR1 (Fig. 3a), and again attenuated β-cat-dependent transcriptional activation (Fig. 3b,c), confirming the primary screen. No effect was observed in control HEK293-Luc cells

(293Luc), a line expressing luciferase from a constitutive non-β-cat-responsive CMV promoter (Fig. 3d).

To independently confirm that the absence of VEGFR1 resulted in attenuated Wnt signaling at the level of transcriptional activation of Wnt/β-cat targets, we obtained embryonic stem (ES) cells derived from a *VEGFR1*$^{(-/-)}$ mouse (18). Importantly, quantitative reverse transcriptase PCR-based profiling for genes implicated in Wnt signaling was performed in both wild type and *VEGFR1*$^{(-/-)}$ ES cells. ES cells lacking *VEGFR1* and treated with rWnt3a showed a mere 5-fold increase in expression of T (Brachyury), a specific transcriptional target of Wnt3a in ES cells (19) ($2^{-\Delta C}$t values: 4.5e-02 (treated) versus 8.6e-03 (untreated)). By comparison, in rWnt3a-treated wild type ES cells, a robust 44-fold increase in T was observed ($2^{-\Delta C}$t values: 6.2e-02 (treated) versus 1.4e-03 (untreated)). These data provided strong evidence that VEGFR1 enhanced Wnt signaling in ES cells.

Inhibition of VEGFR1 tyrosine kinase activity inhibits Wnt/β-cat-dependent transcription and is synthetic lethal in colon cancer cells

Recent data indicate that the expression of VEGFR1 in primary colon carcinoma tumor samples correlates with disease progression (20). However, the mechanistic basis of this observation has not been elucidated. Thus, to directly test the effect of abrogating VEGFR-TK activity on cell survival, SW480 and KM12L4a cells, colon cancer lines that show constitutive β-cat activation (21), were treated with VEGFR-TK inhibitor II (22) (Inh II) for 72 hrs (Fig. 4a). An Inh II-induced decrease in the MTS cell viability assay was seen in these Wnt/β-cat-addicted colon cancer cells in a concentration-dependent manner. The observed IC_{50} of 336 nM (for SW480) and 120 nM (for KM12L4a) matched the known IC_{50} for inhibition of VEGFR1-TK activity (180 nM), a value 9-fold greater than the IC_{50} for inhibition of VEGFR2-TK activity (20 nM) (22). In contrast, a 72 hr MTS assay with STF293 cells, a line that exhibits normal Wnt signaling, was unaffected by Inh II, even in the presence of Wnt stimulation. Furthermore, cervical carcinoma-derived HeLa cells, a line that does not exhibit aberrant Wnt/β-cat pathway activation (23), also showed no response to Inh II (Fig. 4a). These data suggested that VEGFR-TK inhibition was synthetic lethal to cells with aberrant Wnt/β-cat signaling, a process essential for colon cancer cell survival (24), but not to cells with normal Wnt/β-cat signaling. However, further analysis of the luciferase transcriptional reporter showed that treatment with Inh II still resulted in a concentration-dependent inhibition of canonical β-cat-dependent transcription in STF293 cells (Fig. 4b), but only in the presence of Wnt3a, as confirmed by transient transfection of HEK293T cells with *pTOPFLASH*, a similar β-cat-dependent bioluminescence reporter as used in STF293 cells (Fig. 4b, *Inset*). Finally, in SW480 and KM12L4a colon cancer cells transiently transfected with the *pTOPFLASH* reporter, constitutively active β-cat-dependent transcription was also attenuated upon treatment with Inh II (Fig. 4c). These effects were recapitulated with VEGFR-TK inhibitor III, a second inhibitor targeting VEGFR-TK activity (25) (Supplementary Fig. 3a, b), but no effects were observed in off-target transcriptional reporter cells (293Luc), as expected (data not shown). Thus, while inhibition of VEGFR1-TK activity blocked Wnt-induced β-cat-dependent transcription in normal cells as well as constitutively active β-cat-dependent transcription in colon cancer cells, only in colon cancer cells was VEGFR1-TK blockade lethal. Overall, with the caveat that the pharmacological specificity of the tested inhibitors is not fully resolved, these data showed that by targeting VEGFR1-TK activity, the therapeutically-exploitable vulnerability of "Wnt/β-cat-addicted" colon carcinoma was exposed.

Wnt pathway modulation by VEGFR1 is independent of GSK3β-dependent β-cat stabilization

Mutations in APC or β-cat are prevalent in colon carcinoma, resulting in constitutively-stabilized β-cat that is no longer a substrate for GSK3β (1,2). Concordantly, in STF293 cells in which β-cat was stabilized by pharmacological treatment with the GSK3β inhibitor

SB216763 (10 μM) (26), knock-down of VEGFR1 with duplexes of siRNA yielded a similar attenuation of β-cat-dependent transcription (Fig. 5a) as VEGFR1 knock-down in the context of Wnt3a stimulation (Fig. 3c) . Thus, the effect of VEGFR1 was independent of GSK3β.

Downstream Processing

VEGFR1 did not appear to impact processing of total β-cat protein levels. For example, Western blot analysis of STF293 cells showed competent stabilization of β-cat protein upon stimulation with Wnt3a, even when effective knock-down of VEGFR1 protein was achieved with siRNA (Fig. 5b) or VEGFR-TK activity was blocked (Fig. 5c). Overall, these data would suggest that therapeutic interventions directed at VEGFR-TK activity may be mechanistically impacting downstream processing nodes of the Wnt/ β-cat pathway within cells, such as nuclear translocation or transcriptional activation.

We thus explored the effect of VEGFR1 on nuclear translocation of β-cat using immunofluorescence microscopy. In STF293 cells, both VEGFR1 knock-down with siRNA (Fig. 6a) or pharmacological inhibition of VEGFR-TK activity with Inh II (Fig. 6b) resulted in normal Wnt-induced β-cat accumulation and nuclear translocation. These data concurred with observations in $Apc^{Min/+}$ mice that showed no change in nuclear β-cat upon treatment with the VEGFR-TK inhibitor AZD2171 (27). Together, the above observations suggested that regulation of Wnt/β-cat signaling by VEGFR1 occurred at the level of post-translational modification of β-cat as a transcriptional co-regulator and/or subsequent transcriptional activation of a selected subset of β-cat targets.

Preliminary support for VEGFR1-linked effects on post-translational modification of β-cat was provided by analysis of KM12L4a and SW480 colon cancer cells. Inhibition of VEGFR-TK activity by treatment with Inh II, followed by immunoprecipitation and Western blot analysis of β-cat in both lines, showed a dramatic decrease in tyrosine phosphorylated β-cat. However, β-cat total protein levels, which are canonically governed by phospho-serine/ threonine-dependent proteasomal degradation, were found to be unchanged (Fig. 6c). Thus, inhibition of VEGFR1-TK activity resulted in decreased tyrosine phosphorylation of β-cat, thereby abrogating Wnt/β-cat-dependent pro-proliferative transcriptional activity in colon carcinoma cells *per se*.

Discussion

A systematic, yet unbiased screening approach in the context of activated Wnt signaling in human cells has enabled discovery of novel candidate kinase regulators of the Wnt/β-cat pathway. While the Wnt pathway has been extensively pursued using model organism-based genetic screens, recent observations have found newer positive functions of two classic negative regulators of the Wnt pathway, APC (28) and GSK3β (29), highlighting the inherent epistatic bias of conventional assays (30). By interrogating Wnt signaling at the level of transcriptional activation in human STF293 cells using targeted RNA interference, we hoped to identify novel candidate repressors as well as activators of the Wnt/β-cat pathway, which could be further interrogated in cell-specific contexts. Additionally, when establishing a screening strategy, there may be concern that the multitude of altered functional pathways and additional dysregulated kinases in colon cancer cell lines could confound discovery of Wnt pathway-specific regulators. For a conventional synthetic lethal assay, we reasoned that the likelihood was high that a siRNA library screen would identify candidates that simply killed colon cancer cells via other pathways, and hence would give rise to off-target effects instead of direct effects on Wnt-dependent transcription. Thus, by starting with STF293 cells, we demonstrated that one identified candidate, VEGFR1/Flt1, was a regulatory target with clinical relevance, by examining Wnt/β-cat-dependent transcription in a wide variety of contexts, including genetic-null embryonic cells from a $VEGFR1^{-/-}$ mouse, loss-of-function by siRNA

and shRNA, VEGFR-TK inhibition in Wnt-responsive cells, as well as survival of Wnt/β-cat-addicted colon carcinoma cells.

Our data provide potential mechanistic linkages in support of prior observations. For example, VEGFR1 is expressed on various colon cancer lines that show activated Wnt signaling, including SW480 and KM12L4a cells (21). In addition, preclinical studies of a hexapeptide specifically targeting VEGFR1 (31), as well as the VEGFR tyrosine kinase (VEGFR-TK) inhibitors SU11248 (32), AZD2171 (27), and CHIR-258 (33), have shown efficacy in various models of colon cancer, but whether the mechanism involved therapeutic "anti-angiogenesis" remains unclear (21). Furthermore, we found that VEGFR1-linked regulation of β-cat was found to be independent of GSKβ activity and β-cat nuclear translocation, while impacting β-cat tyrosine phosphorylation, thus providing preliminary insight into a mechanism for the anti-proliferation action of VEGFR1 inhibition. It is acknowledged that the exact site of tyrosine phosphorylation remains to be mapped, and the potential differential roles of soluble-VEGFR1, a splice variant (34), versus full length VEGFR1 need to be resolved. Nonetheless, the implication that VEGFR1 links tyrosine kinase activity, directly or indirectly, to a node of the Wnt pathway downstream of commonly occurring oncogenic mutations tremendously enhances its potential as a therapeutic target in the context of aberrant Wnt signaling in cancer.

Our siRNA-based high throughput screen, which uncovered an unanticipated tumor cell linkage between VEGFR1 and Wnt/β-cat, extends the context-dependent crosstalk identified between the oncogenic Flt3 and Wnt pathways in acute myeloid leukemia (35) to VEGFR1/Flt1 and Wnt/β-cat in colon carcinoma. Indeed, comparative genomic hybridization analysis of metastatic human colon cancer shows gain of chromosomes 1p, 8q, 13q and 20q, including a distinct amplicon ranging from 13q11 to 13q21 (36), a region that overlaps with the exact cytogenetic location of VEGFR1. Thus, our results provide an alternative tumor cell-centric basis for the partial successes of "anti-angiogenic" therapy being delimited to only a few cancer types, such as colorectal cancer, a Wnt/β-cat-addicted tumor type. Future studies will be pursued to confirm this in clinical specimens in the context of targeted therapy. Potentially, a mechanistically rational strategy for synthetic lethal therapy in the treatment of colon carcinoma is selective and targeted suppression of VEGFR1-TK activity in the Wnt/β-cat-addicted tumor cells themselves.

Statement of Translational Relevance

Activation of Wnt signaling, which is observed constitutively in most colon cancers, targets over 50 genes by a transactivator complex comprising β-cat and T-cell factor (TCF). To uncover novel kinases that modulate Wnt signal transduction and are essential to the survival of cells addicted to Wnt/β-cat signaling, we systematically inactivated, one at a time, all human genes that direct the synthesis of kinases in cells stimulated with Wnt. Our screen identified an unanticipated mode of crosstalk between VEGFR1/Flt1 and the Wnt/β-cat pathway, two pathways of tremendous importance in cancer. Initial mechanistic studies provided evidence for VEGFR1/Flt1-linked tyrosine phosphorylation of β-cat, thereby modifying transcriptional activity. Thus, a mechanistically rational strategy for synthetic lethal therapy in the treatment of colon carcinoma is targeted suppression of VEGFR1-linked tyrosine kinase activity within the Wnt/β-cat-addicted tumor cell compartment *per se*, not endothelia.

Supplementary Material

Refer to Web version on PubMed Central for supplementary material.

Acknowledgments

The authors would like to thank Dr. D. Maxwell for assistance with immunofluorescence microscopy, Dr. J. Hsieh for assistance with RT-PCR profiling, and colleagues at the Washington University Molecular Imaging Center for discussion. This work was supported by NIH Grant P50 CA94056 (D.P.-W.), the Siteman Cancer Center at Washington University School of Medicine through an NCI Cancer Center Support Grant (P30 CA091842) and an Anheuser-Busch/Emerson Challenge Gift, the Cancer Biology Pathway training program through the Siteman Cancer Center (S.N.), and an American Cancer Society Postdoctoral Fellowship (R.S.D.).

References

1. Giles RH, van Es JH, Clevers H. Caught up in a Wnt storm: Wnt signaling in cancer. Biochim Biophys Acta 2003;1653:1–24. [PubMed: 12781368]
2. Clevers H. Wnt/beta-catenin signaling in development and disease. Cell 2006;127:469–80. [PubMed: 17081971]
3. Kaelin WG Jr. The concept of synthetic lethality in the context of anticancer therapy. Nat Rev Cancer 2005;5:689–98. [PubMed: 16110319]
4. Willingham AT, Deveraux QL, Hampton GM, Aza-Blanc P. RNAi and HTS: exploring cancer by systematic loss-of-function. Oncogene 2004;23:8392–400. [PubMed: 15517021]
5. Hartman JT, Garvik B, Hartwell L. Principles for the buffering of genetic variation. Science 2001;291:1001–4. [PubMed: 11232561]
6. Friend S, Oliff A. Emerging uses for genomic information in drug discovery. N Engl J Med 1998;338:125–6. [PubMed: 9420347]
7. Gross S, Piwnica-Worms D. Real-time imaging of ligand-induced IKK activation in intact cells and in living mice. Nat Methods 2005;2:607–14. [PubMed: 16094386]
8. Zhang XD, Yang XC, Chung N, et al. Robust statistical methods for hit selection in RNA interference high-throughput screening experiments. Pharmacogenomics 2006;7:299–309. [PubMed: 16610941]
9. Xu Q, Wang Y, Dabdoub A, et al. Vascular development in the retina and inner ear: control by Norrin and Frizzled-4, a high-affinity ligand-receptor pair. Cell 2004;116:883–95. [PubMed: 15035989]
10. Shibamoto S, Higano K, Takada R, et al. Cytoskeletal reorganization by soluble Wnt-3a protein signalling. Genes Cells 1998;3:659–70. [PubMed: 9893023]
11. DasGupta R, Kaykas A, Moon RT, Perrimon N. Functional genomic analysis of the Wnt-wingless signaling pathway. Science 2005;308:826–33. [PubMed: 15817814]
12. Ma Y, Creanga A, Lum L, Beachy PA. Prevalence of off-target effects in Drosophila RNA interference screens. Nature 2006;443:359–63. [PubMed: 16964239]
13. Firestein R, Bass A, Kim S, et al. CDK8 is a colorectal cancer oncogene that regulates beta-catenin activity. Nature 2008;455:547–51. [PubMed: 18794900]
14. Weinstein IB, Joe AK. Mechanisms of disease: Oncogene addiction--a rationale for molecular targeting in cancer therapy. Nat Clin Pract Oncol 2006;3:448–57. [PubMed: 16894390]
15. de Vries C, Escobedo JA, Ueno H, et al. The fms-like tyrosine kinase, a receptor for vascular endothelial growth factor. Science 1992;255:989–91. [PubMed: 1312256]
16. Shibuya M. Vascular endothelial growth factor receptor-1 (VEGFR-1/Flt-1): a dual regulator for angiogenesis. Angiogenesis 2006;9:225–30. discussion 31. [PubMed: 17109193]
17. Jain RK, Duda DG, Clark JW, Loeffler JS. Lessons from phase III clinical trials on anti-VEGF therapy for cancer. Nat Clin Pract Oncol 2006;3:24–40. [PubMed: 16407877]
18. Fong GH, Rossant J, Gertsenstein M, Breitman ML. Role of the Flt-1 receptor tyrosine kinase in regulating the assembly of vascular endothelium. Nature 1995;376:66–70. [PubMed: 7596436]
19. Arnold SJ, Stappert J, Bauer A, et al. Brachyury is a target gene of the Wnt/beta-catenin signaling pathway. Mech Dev 2000;91:249–58. [PubMed: 10704849]
20. Bates RC, Goldsmith JD, Bachelder RE, et al. Flt-1-dependent survival characterizes the epithelial-mesenchymal transition of colonic organoids. Curr Biol 2003;13:1721–7. [PubMed: 14521839]
21. Fan F, Wey JS, McCarty MF, et al. Expression and function of vascular endothelial growth factor receptor-1 on human colorectal cancer cells. Oncogene 2005;24:2647–53. [PubMed: 15735759]

22. Furet P, Bold G, Hofmann F, et al. Identification of a new chemical class of potent angiogenesis inhibitors based on conformational considerations and database searching. Bioorg Med Chem Lett 2003;13:2967–71. [PubMed: 12941313]
23. Mikheev AM, Mikheeva SA, Liu B, Cohen P, Zarbl H. A functional genomics approach for the identification of putative tumor suppressor genes: Dickkopf-1 as suppressor of HeLa cell transformation. Carcinogenesis 2004;25:47–59. [PubMed: 14555616]
24. Verma UN, Surabhi RM, Schmaltieg A, Becerra C, Gaynor RB. Small interfering RNAs directed against beta-catenin inhibit the in vitro and in vivo growth of colon cancer cells. Clin Cancer Res 2003;9:1291–300. [PubMed: 12684397]
25. Nakamura K, Yamamoto A, Kamishohara M, et al. KRN633: A selective inhibitor of vascular endothelial growth factor receptor-2 tyrosine kinase that suppresses tumor angiogenesis and growth. Mol Cancer Ther 2004;3:1639–49. [PubMed: 15634658]
26. Cross DA, Culbert AA, Chalmers KA, et al. Selective small-molecule inhibitors of glycogen synthase kinase-3 activity protect primary neurones from death. J Neurochem 2001;77:94–102. [PubMed: 11279265]
27. Goodlad RA, Ryan AJ, Wedge SR, et al. Inhibiting vascular endothelial growth factor receptor-2 signaling reduces tumor burden in the ApcMin/+ mouse model of early intestinal cancer. Carcinogenesis 2006;27:2133–9. [PubMed: 16782971]
28. Takacs CM, Baird JR, Hughes EG, et al. Dual positive and negative regulation of wingless signaling by adenomatous polyposis coli. Science 2008;319:333–6. [PubMed: 18202290]
29. Zeng X, Huang H, Tamai K, et al. Initiation of Wnt signaling: control of Wnt coreceptor Lrp6 phosphorylation/activation via frizzled, dishevelled and axin functions. Development 2008;135:367–75. [PubMed: 18077588]
30. Huang H, He X. Wnt/beta-catenin signaling: new (and old) players and new insights. Curr Opin Cell Biol. 2008
31. Bae DG, Kim TD, Li G, Yoon WH, Chae CB. Anti-flt1 peptide, a vascular endothelial growth factor receptor 1-specific hexapeptide, inhibits tumor growth and metastasis. Clin Cancer Res 2005;11:2651–61. [PubMed: 15814646]
32. Mendel DB, Laird AD, Xin X, et al. In vivo antitumor activity of SU11248, a novel tyrosine kinase inhibitor targeting vascular endothelial growth factor and platelet-derived growth factor receptors: determination of a pharmacokinetic/pharmacodynamic relationship. Clin Cancer Res 2003;9:327–37. [PubMed: 12538485]
33. Lee SH, Lopes de Menezes D, Vora J, et al. In vivo target modulation and biological activity of CHIR-258, a multitargeted growth factor receptor kinase inhibitor, in colon cancer models. Clin Cancer Res 2005;11:3633–41. [PubMed: 15897558]
34. Huckle WR, Roche RI. Post-transcriptional control of expression of sFlt-1, an endogenous inhibitor of vascular endothelial growth factor. J Cell Biochem 2004;93:120–32. [PubMed: 15352169]
35. Kajiguchi T, Chung EJ, Lee S, et al. FLT3 regulates beta-catenin tyrosine phosphorylation, nuclear localization, and transcriptional activity in acute myeloid leukemia cells. Leukemia. 2007
36. Platzer P, Upender MB, Wilson K, et al. Silence of chromosomal amplifications in colon cancer. Cancer Res 2002;62:1134–8. [PubMed: 11861394]

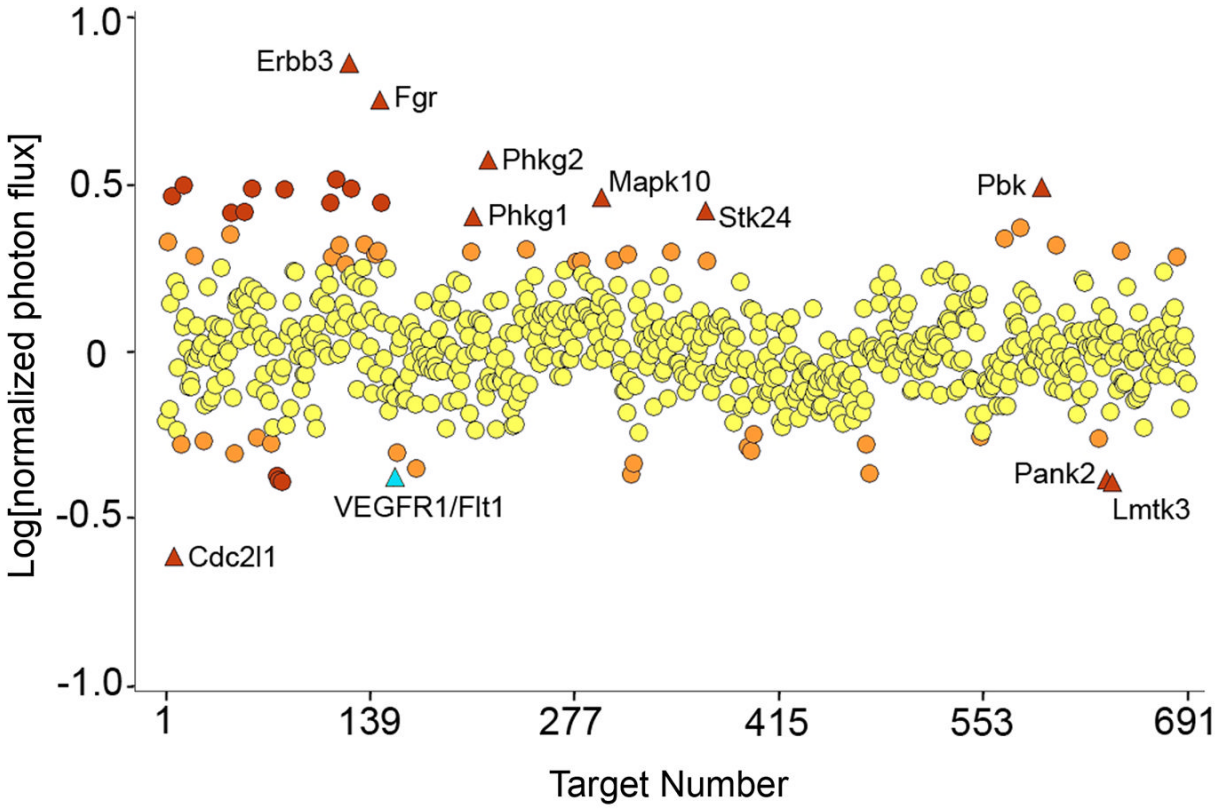

Figure 1. High-throughput RNA interference screen for kinase modulators of Wnt signaling

Screen results including "hits" at various significance thresholds. Log[normalized photon flux] represents bioluminescence reporter signal intensity normalized for cell viability and a control non-targeting sequence placed on each plate to facilitate experiment-wide analysis. Values are plotted for siRNA against all 691 kinase targets. Log[normalized photon flux] values of < -0.37 and > 0.38 score as significant by high stringency criteria ($\alpha \leq 0.0027$) and are indicated in red. Values that lie between -0.37 and -0.25 and between 0.38 and 0.26 score as significant by lower stringency criteria ($\alpha \leq 0.046$) and are indicated in orange. "Hits" that scored at $\alpha \leq 0.0027$ in both an experiment-wide and plate-by-plate analysis are indicated as red triangles (see Supplementary Table 1), and VEGFR1/Flt1 by a blue triangle. The cluster of red circles between targets 1-150 represents "hits" that score as significant by high stringency criteria in an experiment-wide analysis only, but not by a plate-by-plate analysis (listed in Supplementary Table 3). For details on the quartile-based statistical analysis see Materials and Methods; siRNA sequences targeting genes identified as high stringency "hits" in the primary screen are listed in Supplementary Table 4.

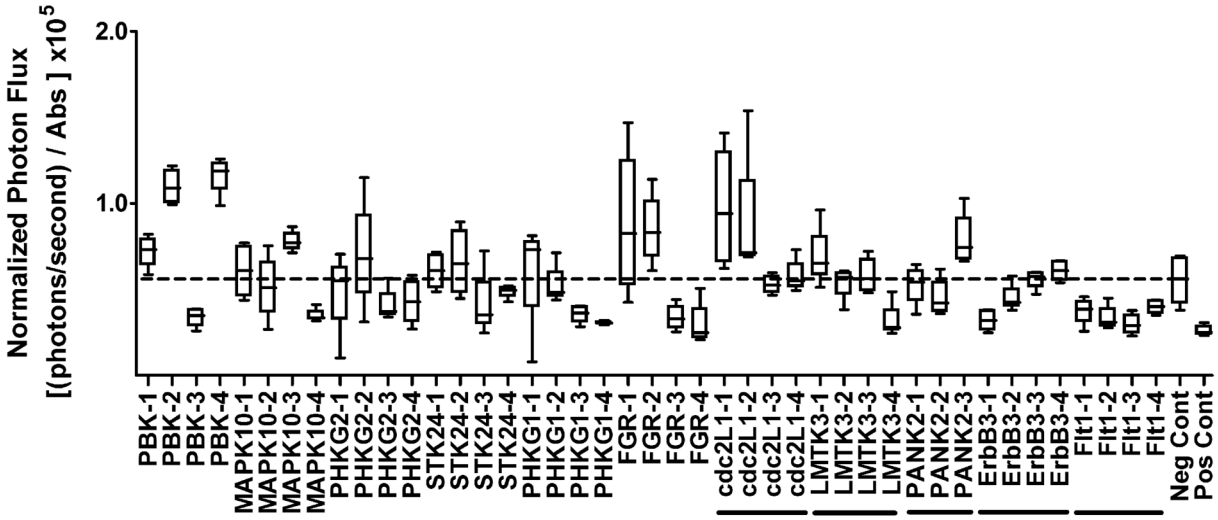

Figure 2. Validation of Wnt/β-cat signaling changes following shRNA knock-down of "hits"

Box and whisker plot of one representative experiment demonstrating luciferase reporter signal changes in STF293 cells 48 hrs after transfection with shRNA plasmids. Four different shRNA sequences targeting non-overlapping segments of the coding regions of the indicated genes were tested in quadruplicate (x-axis). Photon flux in each well was normalized for cell viability (Abs). Lines represent medians, boxes represent 25th to 75th percentile interquartile ranges, and whiskers represent the highest and lowest values for each replicate within a given gene. The dashed horizontal line represents the median value of a negative control. Genes reproducible across at least two of three independent experiments are indicated by an underline.

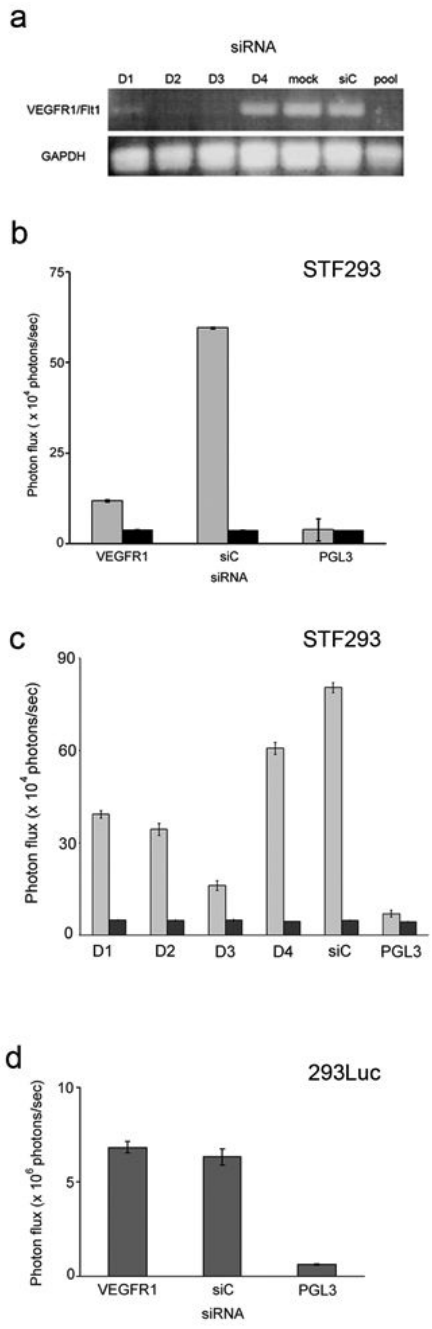

Figure 3. Validation of negative regulation of Wnt/β-cat signaling upon loss of VEGFR1 using pooled and individual siRNA duplexes targeting VEGFR1

(**a**) Gel electrophoresis following semi-quantitative RT-PCR from STF293 cells mock transfected (mock) or transfected with individual duplexes (D1-D4) targeting VEGFR1, a non-targeting siCONTROL sequence (siC), or a set of 4 pooled ON-TARGET plus sequences against VEGFR1 (pool). Gene-specific primers were used to amplify VEGFR1 or control GAPDH. Effect of (**b**) a set of 4 pooled siRNA sequences against VEGFR1, or (**c**) individual sequences (D1-D4) targeting VEGFR1, along with non-targeting siC as well as a Firefly luciferase (PGL3)-targeting siRNA on STF293 cells stimulated with Wnt3a (gray) or control media (black). Data are represented as mean photon flux +/− S.E.M (n=3 per condition). (**d**)

Knock-down of VEGFR1 had no effect on control 293Luc cells expressing a non-Wnt-dependent reporter, both in the absence (shown) or presence of Wnt3a.

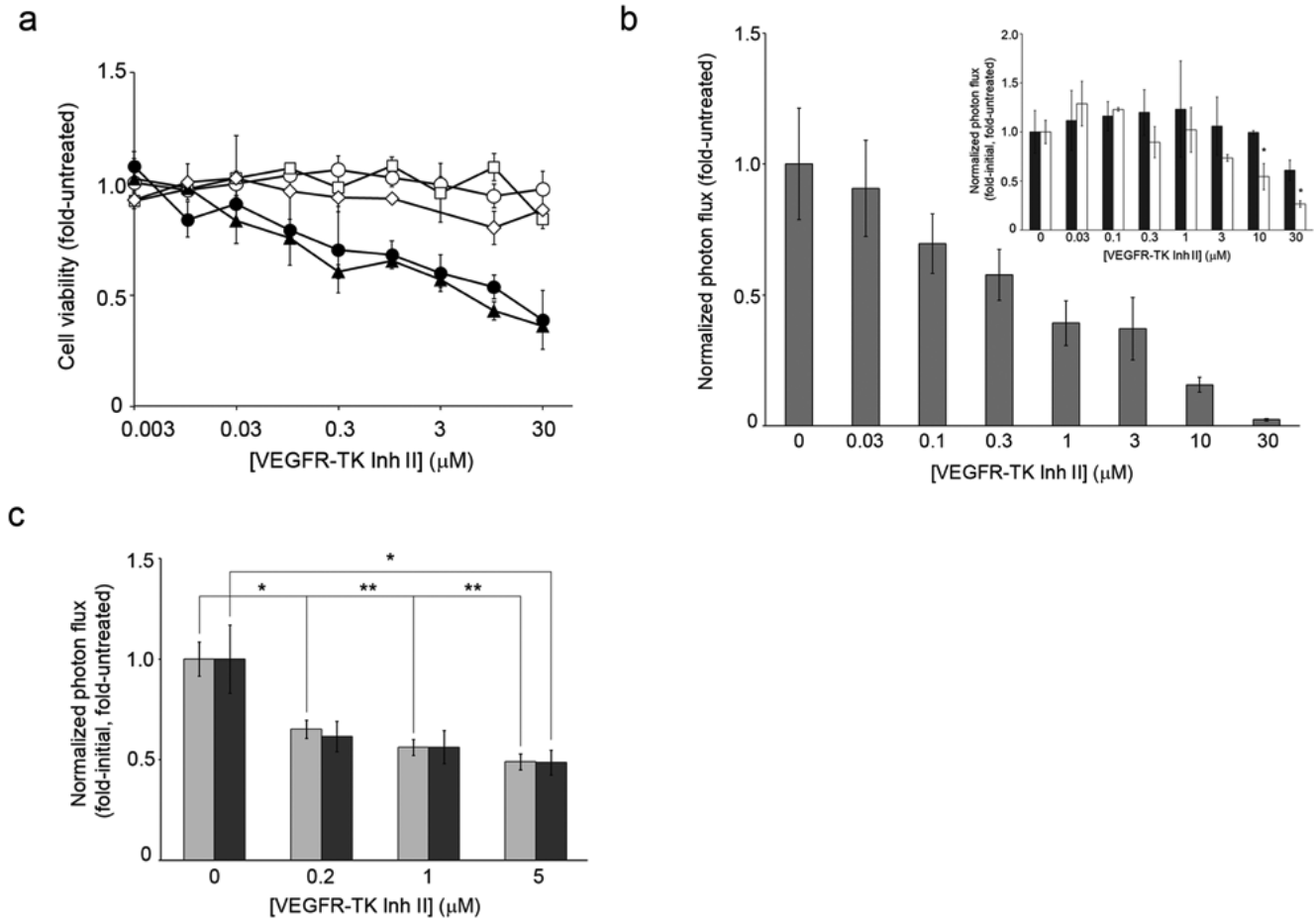

Figure 4. Inhibition of VEGFR tyrosine kinase activity is synthetic lethal in "β-cat-addicted" colon cancer cells, acting through downregulation of Wnt/β-cat-dependent transcriptional activation

(**a**) Inhibition of VEGFR-TK activity selectively diminishes viability of SW480 (solid circle) and KM12L4a (solid triangle) colon cancer cells, but not Wnt3a-stimulated STF293 cells (open square), control STF293 cells (open diamond) or non-colon cancer HeLa cells (open circle). Each cell type was treated with increasing concentrations of Inh II for 72 hrs before cell viability analysis using an MTS assay. Data are represented as mean +/− S.E.M. of fold-untreated absorbance values from two independent experiments (n=3 each) for each concentration for each cell line. (**b**) Reporter concentration-response in STF293 cells stimulated with Wnt3a following pre-treatment with increasing concentrations of Inh II. Bioluminescence photon flux was normalized to cell viability using a resazurin dye-based fluorescence assay and plotted as fold-untreated normalized photon flux +/− propagated S.E.M. (n=3 per concentration). (***Inset***) In HEK293T cells transfected with *pTOPFLASH*, Inh II strongly attenuated β-cat-dependent transcription induced by Wnt3a (white bars), but showed a statistically significant lower effect on basal transcriptional activity in the absence of Wnt3a (black bars). Bioluminescence photon flux was normalized to cell viability using a resazurin dye-based fluorescence assay and plotted as fold-initial, fold-untreated normalized photon flux +/− propagated S.E.M. (n=3 per concentration). Statistical significance by Student's *t*-test is indicated as * ($p < 0.05$). A two-way analysis of variance also found statistically significant effects of both Wnt treatment ($p < 0.05$) and drug concentration ($p < 0.001$). (**c**) Inhibitory effect of a 48-hour exposure to increasing concentrations of Inh II on constitutively active β-cat-dependent signaling in SW480 (gray bars) and KM12L4a (black bars) colon carcinoma cells

transfected with *pTOPFLASH*. Data are represented as mean fold-initial, fold-untreated photon flux +/− propagated S.E.M. (n= 3 per concentration). Statistical significance by Student's *t*-test is indicated as * ($p < 0.05$) and ** ($p < 0.01$).

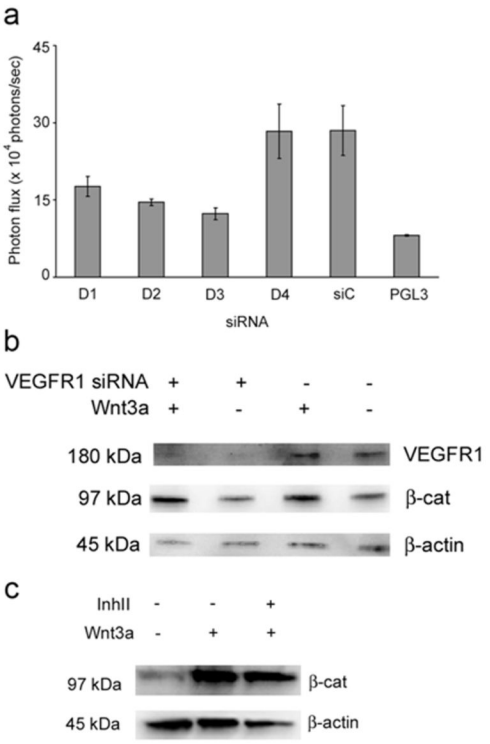

Figure 5. VEGFR1 acts in a GSK3β-independent manner and downstream of β-cat protein stabilization

(**a**) Effects of individual duplexes (D1-D4) targeting VEGFR1, a non-targeting siCONTROL sequence (siC) and a Firefly luciferase-targeting (PGL3) siRNA on STF293 cells treated with the GSK3β inhibitor SB216763 (10 μM). Bioluminescence photon flux is represented as mean photon flux +/− S.E.M. (n=4). (**b**) Western Blot analysis of STF293 cells transfected with ON-TARGET plus SMARTpool siRNA targeting VEGFR1 (Lanes 1 & 2) or off-target PGL3-targeting siRNA (Lanes 3 & 4), and stimulated with Wnt3a (Lanes 1 & 3) or control media (Lanes 2 & 4), or (**c**) treated with vehicle (Lanes 1 & 2) or 1 μM VEGFR-TK Inh II (Lane 3) for 18 hrs together with control media (Lane 1) or Wnt3a (Lanes 2 & 3).

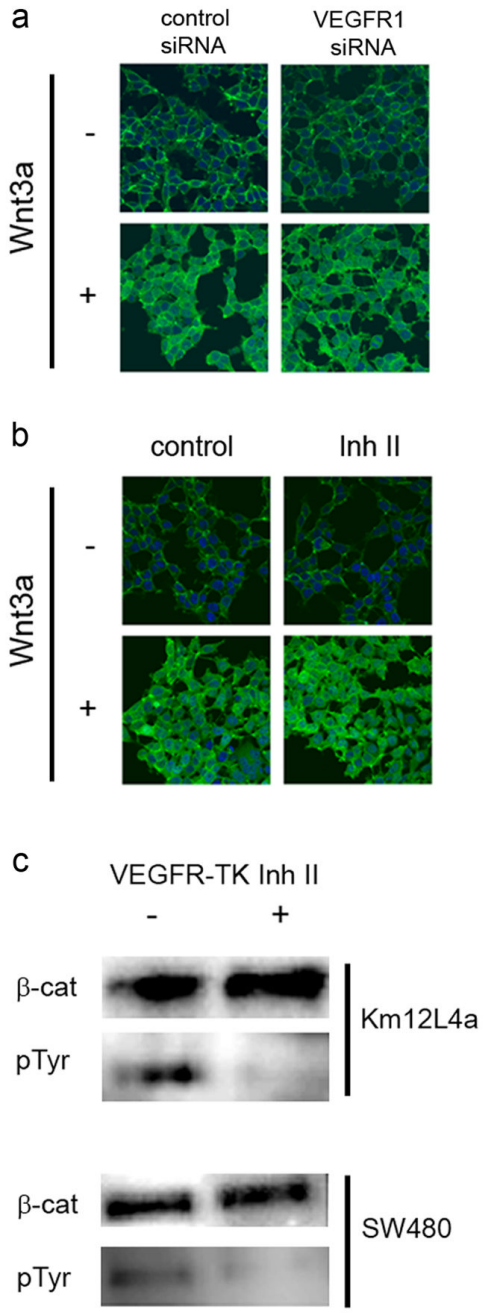

Figure 6. Modulation of Wnt/β-cat signaling by VEGFR1 is independent of β-cat stabilization and nuclear translocation, but correlates with β-cat tyrosine phosphorylation

(**a**, **b**) Confocal immunofluorescence microscopy images showing β-cat subcellular localization (green) in STF293 cells transfected with either siRNA targeting VEGFR1 or a non-targeting control duplex for 48 hrs (a) or treated with Inh II (1 μM) or vehicle for 18 hrs (b). Cells were stimulated for two hours with either control media (top) or Wnt3a (bottom). Nuclei (blue) were stained with DAPI (magnification 40X). (**c**) Western blot analysis of immunoprecipitated β-cat from KM12L4a and SW480 colon carcinoma cells treated with Inh II (1 μM) for 48 hrs. Samples were first probed with anti-phospho tyrosine (pTyr) antibody, stripped and reprobed with anti-β-cat antibody.